Deep Learning Assisted Classification of T1ρ-MR Based Intervertebral Disc Degeneration Phases

Yanrun Li, MS,[1] Meiyu Hu, MS,[2,3,4] Junhong Chen, BMed,[5] Zemin Ling, PhD,[1,6] Xuenong Zou, PhD,[6] Wuteng Cao, PhD,[2,3,4*] and Fuxin Wei, PhD[1*]

Background: According to the T1ρ value of nucleus pulposus, our previous study has found that intervertebral disc degeneration (IDD) can be divided into three phases based on T1ρ-MR, which is helpful for the selection of biomaterial treatment timing. However, the routine MR sequences for patients with IDD are T1- and T2-MR, T1ρ-MR is not commonly used due to long scanning time and extra expenses, which limits the application of T1ρ-MR based IDD phases.
Purpose: To build a deep learning model to achieve the classification of T1ρ-MR based IDD phases from routine T1-MR images.
Study Type: Retrospective.
Population: Sixty (M/F: 35/25) patients with low back pain or lower limb radiculopathy are randomly divided into training (N = 50) and test (N = 10) sets.
Field Strength/Sequences: 1.5 T MR scanner; T1-, T2-, and T1ρ-MR sequence (spin echo).
Assessment: The T1ρ values of the nucleus pulposus in intervertebral discs (IVDs) were measured. IVDs were divided into three phases based on the mean T1ρ value: pre-degeneration phase (mean T1ρ value >110 msec), rapid degeneration phase (mean T1ρ value: 80–110 msec), and late degeneration phase (mean T1ρ value <80 msec). After measurement, the T1ρ values, phases, and levels of IVDs were input into the model as labels.
Statistical Tests: Intraclass correlation coefficient, area under the receiver operating characteristic curve (AUC), F1-score, accuracy, precision, and recall ($P < 0.05$ was considered significant).
Results: In the test dataset, the model achieved a mean average precision of 0.996 for detecting IVD levels. The diagnostic accuracy of the T1ρ-MR based IDD phases was 0.840 and the AUC was 0.871, the average AUC of 5-folds cross validation was 0.843.
Data Conclusion: The proposed deep learning model achieved the classification of T1ρ-MR based IDD phases from routine T1-MR images, which may provide a method to facilitate the application of T1ρ-MR in IDD.
Evidence Level: 4
Technical Efficacy: Stage 2

J. MAGN. RESON. IMAGING 2024.

It is estimated that about 50%–80% of adults will experience low back pain in their lifetime, which will reduce their quality of life and can cause disability.[1–3] Intervertebral disc degeneration (IDD) is closely related to lower back pain.[4] For patients with severe symptoms and signs who are ineffective in conservative treatment, surgery is the main clinical treatment.[5,6] Although surgery can alleviate the suffering of patients, it is costly and there is a risk of surgical

View this article online at wileyonlinelibrary.com. DOI: 10.1002/jmri.29499

Received Nov 9, 2023, Accepted for publication Jun 7, 2024.

*Address reprint requests to: F.W., No. 628, Zhenyuan Road, Shenzhen, China. E-mail: weifuxin@mail.sysu.edu.cn, or W.C., No. 26, Yuancunerheng Road, Guangzhou, China. E-mail: caowteng@mail.sysu.edu.cn
Yanrun Li, Meiyu Hu, and Junhong Chen contributed equally to this work.

From the [1]Shenzhen Key Laboratory of Bone Tissue Repair and Translational Research, Department of Orthopaedic Surgery, The Seventh Affiliated Hospital, Sun Yat-sen University, Shenzhen, China; [2]Department of Radiology, The Sixth Affiliated Hospital, Sun Yat-sen University, Guangzhou, China; [3]Guangdong Provincial Key Laboratory of Colorectal and Pelvic Floor Diseases, Guangdong Research Institute of Gastroenterology, The Sixth Affiliated Hospital, Sun Yat-sen University, Guangzhou, China; [4]Biomedical Innovation Center, The Sixth Affiliated Hospital, Sun Yat-sen University, Guangzhou, China; [5]School of Public Health (Shenzhen), Shenzhen Campus of Sun Yat-sen University, Shenzhen, China; and [6]Guangdong Provincial Key Laboratory of Orthopedics and Traumatology, Department of Spinal Surgery, The First Affiliated Hospital of Sun Yat-sen University, Guangzhou, China

complications.[7,8] Therefore, early diagnosis of IDD and exploring possible treatment methods are of great importance.

At present, the Pfirmann grading is widely used in the evaluation of IDD. Based on T2-MR images, Pfirmann grading divided intervertebral discs (IVDs) into five grades according to the severity of IDD.[9] However, the Pfirmann grading cannot quantify the degeneration, and T2-MR is not sensitive to the characteristics of early IDD.[10] T1ρ, or spin-lock T1 relaxation time, is the time constant for magnetic relaxation under continuous radiofrequency irradiation and can reflect the interactions between macromolecules (such as proteoglycan) and water.[11,12] Previous studies have found that T1ρ-MR can evaluate the loss of proteoglycans in degenerative cartilage and IVD, T1ρ value is directly related to the proteoglycan content in nucleus pulposus.[13,14] In the process of IDD, the loss of proteoglycan is one of the most important macromolecular biochemical changes in the early stage of IDD.[15] Therefore, T1ρ-MR should be sensitive to the early stages of IDD.

Our previous study found that IDD can be divided into three phases in IDD patients and rhesus monkeys using T1ρ-MR.[16] The mean T1ρ value of nucleus pulposus in healthy IVD was usually greater than 110 msec. After the start of degeneration, the mean T1ρ value rapidly decreased from 110 to 80 msec in 3 months, indicating a rapid degeneration period in the early stage of IDD. After the mean T1ρ value decreased to 80 msec, it tended to be stable.[16] Thus, based on the mean T1ρ values of nucleus pulposus in IVDs, the process of IDD can be divided into three phases: pre-degeneration phase (phase 1, mean T1ρ value >110 msec), rapid degeneration phase (phase 2, mean T1ρ value: 80–110 msec), and late degeneration phase (phase 3, mean T1ρ value <80 msec) (Fig. 1). Our further study found that injecting hydrogel into nucleus pulposus of IVDs during rapid degeneration (phase 2) could effectively restore the degenerative histological morphology and T1ρ values. In contrast, injection during the late degeneration phase loses therapeutic effect. These results imply that the rapid degeneration phase may be the optimal biomaterial treatment timing to reverse the progression of IDD.[17] Therefore, the use of T1ρ-MR to identify the phases of IDD may provide a new therapeutic strategy. However, due to non-standard image acquisition and post-processing methods, as well as long scanning time, T1ρ-MR is not widely used in clinical practice, which limits its application.[18] Therefore, realizing the convenient use of T1ρ-MR based IDD phases in clinical practice is a problem worth studying.

Deep learning is a machine learning method that has emerged in recent years, which can extract image features in a data-driven manner. It has been widely used in medical image processing and classification tasks.[19] T1-MR is a conventional sequence that is widely used for patients with lumbar diseases, which is easily obtainable in clinical practice. Previous studies have found that deep learning methods can achieve functional substitution or image conversion between different imaging examination methods. Jans et al utilized deep learning methods to generate CT images from conventional T1-MR images for the diagnosis of sacroiliitis, the newly generated CT images achieved a diagnostic accuracy of 0.92.[20]

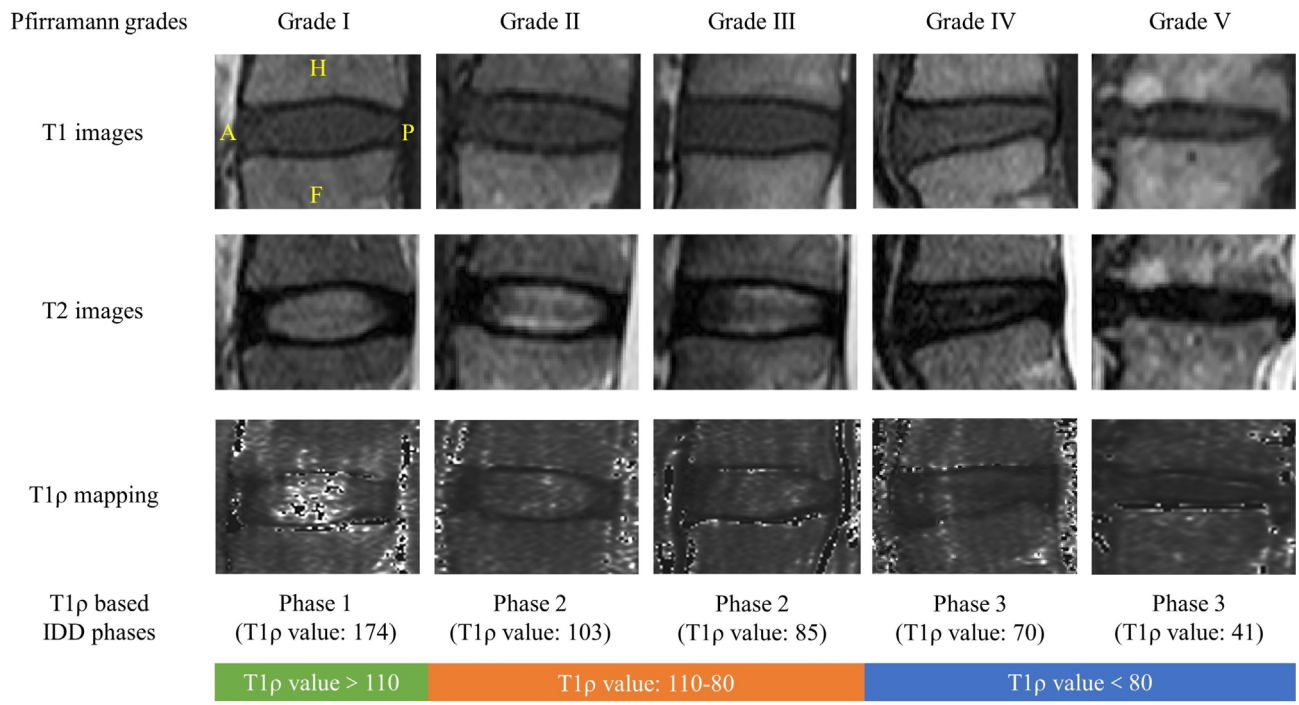

FIGURE 1: T1ρ-MR based IDD phases and corresponding T1 and T2-weighted images. The T1ρ value in this figure refers to the mean T1ρ value. A = anterior; F = feet; H = head; P = posterior.

Moreover, Wu et al found that deep learning methods can be used to generate T1ρ-MR images from T1-MR images.[21] The above studies suggest that deep learning methods provide the possibility of using conventional T1-MR images to achieve the functionality of T1ρ-MR images. Here, we aim to use deep learning method to facilitate the application of T1ρ-MR in IDD evaluation.

Materials and Methods

Study Population

This study was approved by the institutional review board of the First Affiliated Hospital of Sun Yat-sen University (certificate no. [2022]563), informed consent was waived for a retrospective analysis. We collected the data of patients who visited the hospital from January 2010 to May 2010 due to low back pain or lower limb radiculopathy and underwent lumbar spinal T1, T2, and T1ρ-MR. Data regarding sex, age, and MR images were collected. Patients whose MR images have been lost were excluded from the present study, two patients were excluded in total. The final study group consisted of 60 patients (mean age, 36 ± 11 years), including 35 men and 25 women. The patients were divided into a training set (N = 50) and a test set (N = 10) at a ratio of 5:1. As five lumbar IVDs (L1/L2-L5/S1) were analyzed for each patient, 300 IVDs were included in this study, including 250 IVDs in the training set and 50 IVDs in the test set. Other details about the characteristics of patients are listed in Table 1.

TABLE 1. Characteristics of Patients in Datasets

	All Dataset	Training Set	Test Set
Patient	60	50	10
IVD	300	250	50
Sex (Male: Female)	35:25	29:21	6:4
Age (Mean ± SD)	36 ± 11	36 ± 11	37 ± 12
Pfirrmann grade			
Grade I	12	9	3
Grade II	133	107	26
Grade III	83	75	8
Grade IV	68	56	12
Grade V	4	3	1
T1ρ-MR based IDD phase			
Phase 1	144	119	25
Phase 2	76	64	12
Phase 3	80	67	13

IVD = intervertebral disc; SD = standard deviation; IDD = intervertebral disc degeneration.

MR Examination

A 1.5-T MR scanner (Philips Achieva) with a spine-array coil was used for MR scanning. The imaging protocol included multi-section two-dimensional sagittal and axial T1-weighted and T2-weighted fast spin-echo imaging, and a three-dimensional sagittal T1ρ quantification sequence. With spin-lock of 2, 15, 30, and 45 msec, T1ρ-MR images were acquired using spin-lock pulses followed by spin-echo acquisition. The spin-lock frequency is 250 Hz. Our previous research contained details of the MR sequence.[16]

Image Analysis

The MR images were evaluated by a spinal surgeon (2 years experience in evaluation of musculoskeletal images) and a radiologist (23 years experience in evaluation of musculoskeletal images). T1ρ values were calculated using a custom-written program (Siswin, developed by Steffen Ringgaard; MR Research Center at Aarhus University Hospital, Denmark) by fitting the signal intensity data of the spin-lock images to the following exponential function:

$$S(x) = A(x) \cdot e^{\frac{-\mathrm{TSL}}{\mathrm{T1\rho}}(x)},$$

where S is the signal intensity, x is the specific substance, A is the signal intensity when TSL = 0, e is the equilibrium magnetization, and TSL is the spin locking time. After manually selecting the region of interest at the center of the nucleus pulposus (1 cm^2), we measured the maximum, minimum, and mean T1ρ values on the midsagittal T1ρ maps (Fig. 2). To reduce deviation, the spinal surgeon and the radiologist repeated the measurement of T1ρ values three times. The average of the maximum, minimum, and mean T1ρ values was used for IDD phases classification and further training. Based on the mean T1ρ value, the IVDs of L1/L2-L5/S1 were divided into three phases: Phase 1 (mean T1ρ value >110 msec), phase 2 (mean T1ρ value: 80–110 msec), and phase 3 (mean T1ρ value <80 msec). In addition, the Pfirrmann grades of L1/L2-L5/S1 were evaluated by the spinal surgeon and the radiologist according to T2-MR, the inter-observer difference of the Pfirrmann grading was resolved through discussion.[9]

Image Preprocessing and Annotation

The DICOM format T1-MR images were preprocessed with the Insight Segmentation and Registration Toolkit software. The window width was set to 2000, and the window level was set to 1000 for image annotation. We used LabelImg software (Version: 1.8.6, https://github.com/heartexlabs/labelImg) to label IVDs in T1-MR midsagittal images. The regions of five lumbar IVDs (including the nucleus pulposus and annulus fibrosus) of L1/L2-L5/S1 were delineated with rectangular frames, then their levels and T1ρ-MR based IDD phases were labeled. Besides, the measured maximum, minimum and average T1ρ values were also used as labels for model training.

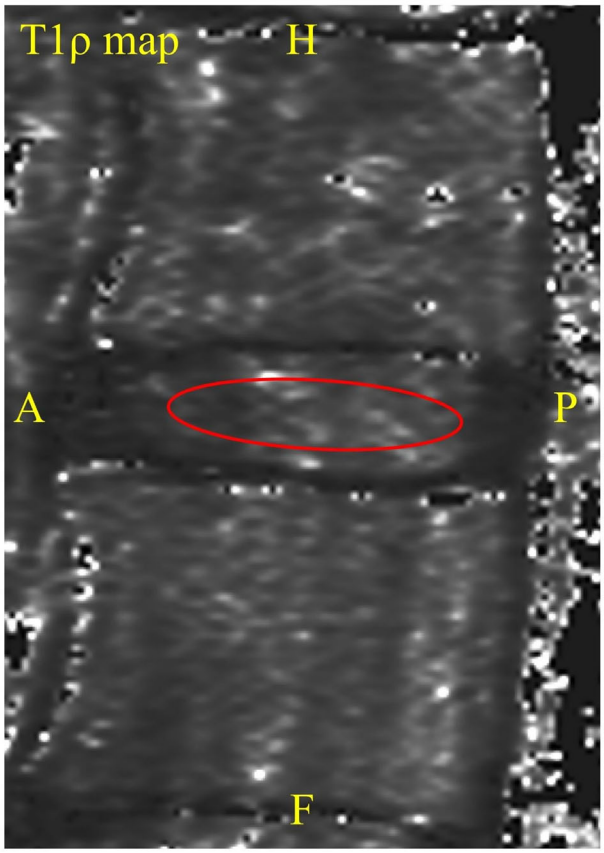

FIGURE 2: Diagram of T1ρ value measurement. 1 cm^2 area at the center of nucleus pulposus was selected in T1ρ map, then maximum, minimum, and mean T1ρ values were calculated within the area. A = anterior; F = feet; H = head; P = posterior.

Deep Learning Algorithm

MODEL ALGORITHMS. In order to classify T1ρ-MR based lumbar IDD phases from routine T1-MR, we developed a novel deep learning model using You Only Look Once version 7 (YOLOv7), wide residual network (WRN), and support vector machine (SVM) frameworks. As shown in Fig. 3, the model can be divided into three stages: IVD detection, output of the T1ρ value feature, and classification of T1ρ-MR based IDD phase. During IVD detection, we developed the function of this stage based on a 314 layers YOLOv7, which was an object detection system that was capable of detecting multiple objects in an image. Then, the images were reshaped to 640 × 640 pixels for training. With precise segmentation of IVDs regions as the input for stage 2, we generated the T1ρ value feature output model based on a 22 layers WRN, which can extract features to output the maximum, minimum and mean T1ρ values from T1-MR images. The last stage was the classification of T1ρ-MR based IDD phases. After stage 2, we obtained the above output T1ρ values as features. In Stage 3, the SVM model used these features for phases classification with a Gaussian kernel.

MODEL DEVELOPMENT. Patients were randomly divided into two datasets: a training set (50 patients, 250 IVDs) and a test set which only used at the end of the process to obtain the final results (10 patients, 50 IVDs) (Fig. 4). The experiments were run on Ubuntu 20.04 with NVIDIA 2080-Ti GPU. The code implementation of the architecture was based on Pytorch 1.10.0 and Sklearn 1.2.1 frameworks in Python 3.7. The IVDs detection model training process was terminated within 200 epochs with a batch size of 16. The T1ρ value feature output model was trained with a learning rate of 1e-4, adaptive moment estimation (Adam) was employed for

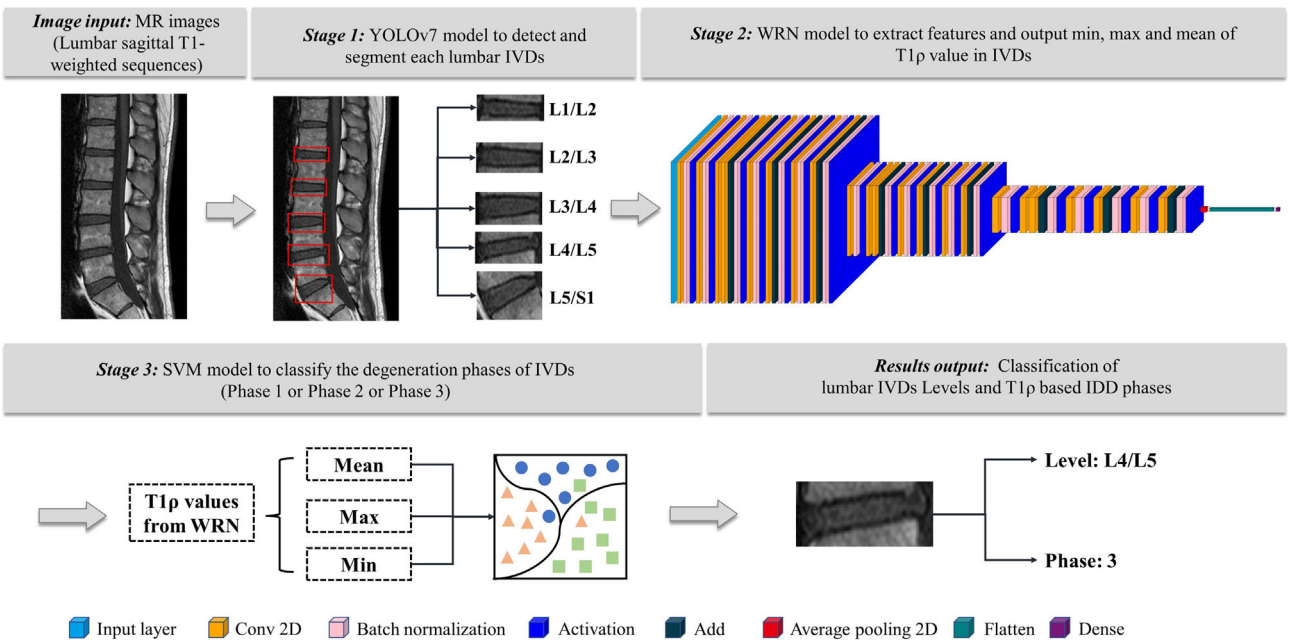

FIGURE 3: Workflow diagram of the YOLOv7-WRN-SVM model. After inputting T1-MR image into the model, YOLOv7 achieves the task of IVD detection. Subsequently, the images of IVD region are segmented and inputted into WRN for feature extraction, then WRN outputs T1ρ values as features. Finally, SVM classifies T1ρ-MR based IDD phases according to these features. IDD = intervertebral disc degeneration; IVD = intervertebral disc; SVM = support vector machine; WRN = wide residual network; YOLO = you only look once.

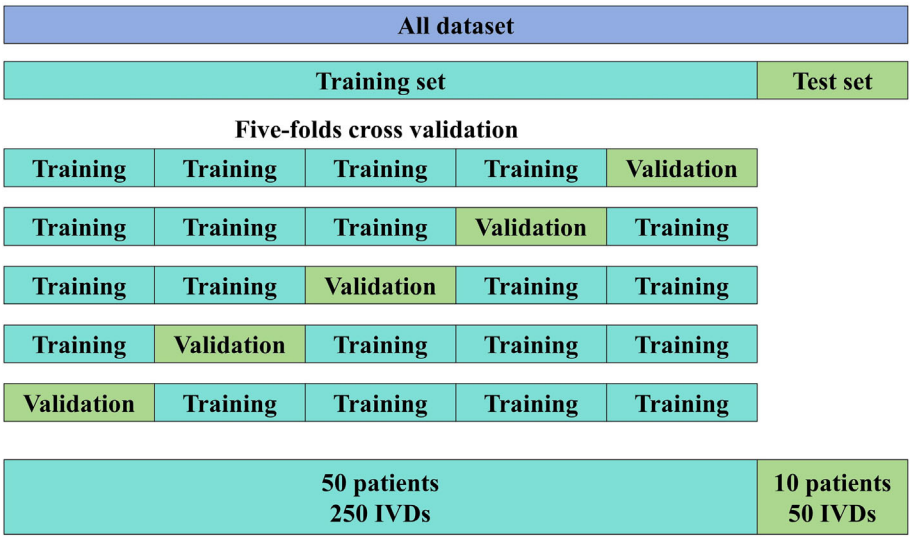

FIGURE 4: Division of the dataset. IVD = intervertebral disc.

optimization. In our training dataset, phase 1 = 119, phase 2 = 64, and phase 3 = 67. To balance our dataset, the synthetic minority oversampling technique (SMOTE) with default parameters was used to equalize the data to the same level (phase 1 = 119, phase 2 = 119, and phase 3 = 119) before phase classification model training.

Statistical Analysis

Quantitative variables are expressed as mean ± SD, and categorical data are expressed as numbers (ratio). For inter- and intra-observer variation in T1ρ values, we used the intraclass correlation coefficient (ICC) for average and single measurements. The reliability of the ICC was rated as follows: 0.00 to 0.10, virtually none; 0.11 to 0.40, slight; 0.41 to 0.60, fair; 0.61 to 0.80, moderate; 0.81 to 1.00, substantial.[22] The inter- and intra-observer analysis of T1ρ values measurement showed substantial reliability with all ICCs greater than 0.80. We evaluated the inter-observer differences in Pfirmann grades using Cohen κ: A κ value less than 0.21 was considered poor agreement; 0.21–0.40, fair agreement; 0.41–0.60, moderate agreement; 0.61–0.80, substantial agreement; and 0.81–1.00, excellent agreement.[23] The κ value of Pfirrmann grades is greater than 0.80, which indicates excellent agreement. The average precision and mean average precision were used to evaluate IVD detection performance. To assess the performance of T1ρ-MR based IDD phases, we used F1-score, accuracy, precision, and recall. A confusion matrix and receiver operating characteristic (ROC) curve were used to visualize the IDD phases classification performance, and we calculated the area under the curve (AUC). In order to further test the stability and reproducibility of the model, we used 5-folds cross validation. The data in training set (50 patients, 250 IVDs) was randomly divided into five equal parts. Four of them were used to train the model and one of them was used to test the model each time (Fig. 4). The above process was repeated five times and the AUC was calculated. To obtain a more accurate evaluation of our results, we employed the bootstrap algorithm, performing 1000 iterations to estimate the 95% confidence interval (CI) for the AUC. Besides, the standard error (SE) of AUC was also calculated. Statistical analyses were conducted using Statistical Product Service Solutions 23 and Python 3.7 software. $P < 0.05$ was considered statistically significant.

Results

The Model Performance of the IVD Detection

Table 2 presents the performance of the YOLOv7 IVD detection model. According to the results, YOLOv7 achieved a mean average precision of 0.996 for segmenting IVD levels in test set. Of the detection for each IVD level, average precision for L1/L2 was 0.996; for L2/L3 was 0.996; for L3/L4 was 0.996; for L4/L5 was 0.995; for L5/S1 was 0.995, respectively. These results showed that IVD detection based on YOLOv7 had excellent performance on lumbar IVDs, which paved the way for the next step of IDD phases classification.

The Model Performance of the T1ρ-MR Based IDD Phase Classification

The diagnostic performance of the model for T1ρ-MR based IDD phase is shown in Table 3. The diagnostic accuracy for

TABLE 2. The Average Precision of the Intervertebral Disc Detection in Test Set

	All Levels	L1/L2	L2/L3	L3/L4	L4/L5	L5/S1
Average precision	0.996[a]	0.996	0.996	0.996	0.995	0.995

[a]Mean average precision.

the IDD phases was 0.840. The recall of phase 2 was significantly higher than those of the other two phases, which allowed the model to identify patients in phase 2 more effectively. The confusion matrices for phases classification were shown in Fig. 5a. The classifier SVM model had an AUC of 0.840 (SE = 0.002, 95% CI: [0.737, 0.926]) for phase 1, 0.906 (SE = 0.001, 95% CI: [0.810, 0.986]) for phase 2, and 0.885 (SE = 0.002, 95% CI: [0.773, 1.000]) for phase 3 (Fig. 5b). The average AUC for the classification of T1ρ-MR based IDD phases was 0.871 (SE = 0.002, 95% CI: [0.769, 0.957]). The further 5-folds cross validation demonstrated the reproducibility of the model with an average AUC of 0.843 (Table 4). The workflow diagram of the YOLOv7-WRN-SVM model was shown in Fig. 6, after inputting sagittal T1-MR image, the model will output levels and T1ρ-MR based IDD phases of lumbar IVDs.

TABLE 3. Precision, Recall, F1-Score, and Accuracy of the T1ρ-MR Based IDD Phase Classification in Test Set

	Precision	Recall	F1-Score	Support
T1ρ based IDD phase				
Phase 1	0.840	0.840	0.840	25
Phase 2	0.733	0.917	0.815	12
Phase 3	1.000	0.769	0.870	13
Accuracy			0.840	50
Macro average	0.858	0.842	0.841	50
Weight average	0.856	0.840	0.842	50

IDD = intervertebral disc degeneration.

Discussion

In this study, we developed the YOLOv7-WRN-SVM model using deep learning method to classify T1ρ-MR based IDD phases from common T1-MR images. Specifically, the model consists of YOLOv7 to tackle the IVD detection task, WRN to extract image features and SVM to classify the IDD phases. The present deep learning model can classify T1ρ-MR based IDD phases from T1-MR images, which may provide a new method for the application of T1ρ-MR in evaluating IDD.

Deep learning has been widely applied to musculoskeletal radiological imaging studies. In the field of IDD, many studies have used this method to assist IDD diagnosis. Niemeyer et al built a model based on deep convolutional neural networks for automatic classification of IDD using Pfirmann grades, and the model achieved an average sensitivity of 0.902 and an average accuracy of 0.925.[24] Zheng et al developed an IVD automated quantitation system that can achieve morphological measurements and Pfirmann grades classification of IVDs.[25] In addition to the widely used Pfirmann grading for IDD, our

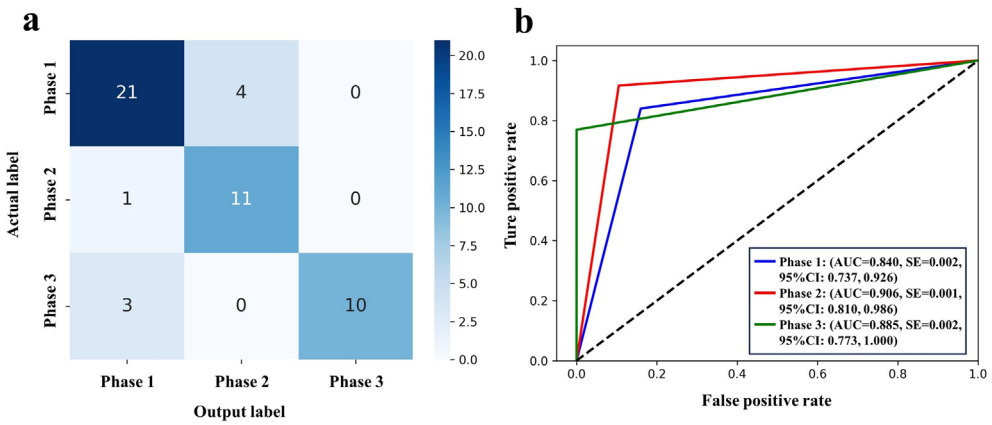

FIGURE 5: Confusion matrix (a) and receiver operating characteristic curve (b) of T1ρ-MR based IDD phase classification in test set. IDD = intervertebral disc degeneration.

TABLE 4. Five-Folds Cross Validation of T1ρ-MR Based IDD Phases for Model Classification

	Five-Folds Cross Validation					
	Average	Fold 1	Fold 2	Fold 3	Fold 4	Fold 5
AUC	0.843	0.796	0.863	0.876	0.815	0.863

AUC = area under the curve.

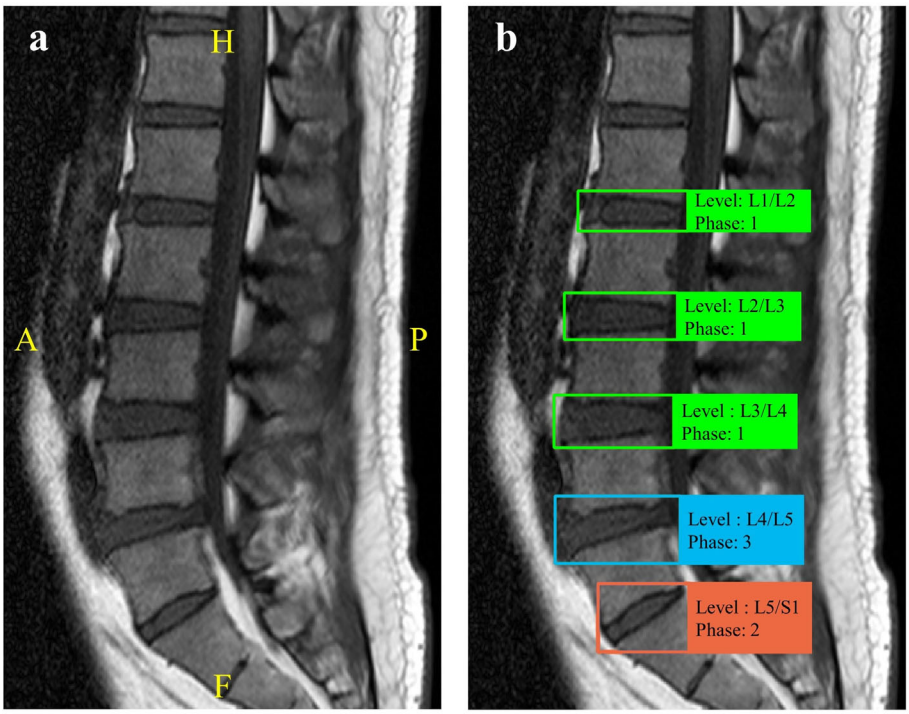

FIGURE 6: Functional diagram of the YOLOv7-WRN-SVM model. (a) Inputting T1-MR image; (b) outputting IVD levels and T1ρ-MR based IDD phases. A = anterior; F = feet; H = head; IDD = intervertebral disc degeneration; P = posterior.

previous study proposed the T1ρ-MR based IDD phases, and subsequent study has found that these phases can assist in the selection of treatment strategies for IDD.[16,17] However, due to nonstandard T1ρ value acquisition and long scanning time, T1ρ-MR is not used as a routine sequence for patients, which limits the application of the T1ρ-MR based IDD phases.[18] At present, studies have found that deep learning method can achieve functional substitution or image conversion between different imaging methods. For example, Fang et al used deep learning to replace the bone mineral density detection function of QCT with CT and achieved high correlation and agreement.[26] Besides, the study of Wu et al found that deep learning can be used to generate T1ρ-MR images through T1-MR images.[21] Therefore, we tried to use deep learning method to classify T1ρ-MR based IDD phases from conventional T1-MR images.

Accurate detection of the IVD regions is the primary condition for the classification of IDD phases. YOLO is a one-stage object detection framework, multiple versions of YOLO have been applied to IVD image learning.[27–29] Tsai et al achieved an accuracy of 0.924 for detecting IVD herniation using YOLOv3.[27] Ito et al built a model using YOLOv4 and achieved automatic detection of spinal tumor using MR images with the accuracy of 0.938.[30] In this study, we used YOLOv7 for IVD detection. The results of the present study showed that the average precision of all five IVDs exceeded 0.995.

WRN is a variant developed on the basis of residual network (ResNet). By making ResNet shallower and wider, WRN can accelerate training speed, reduce computational costs, and improve model performance effectively.[31] Previous studies have combined deep learning algorithms such as ResNet with SVM to achieve better performance. Zhou et al built a model by combining ResNet and SVM. They used chest X-ray images to automatically diagnose pneumonia and achieved an accuracy of 0.930 with a small data set, which was superior to the performance of using ResNet alone.[32] Moreover, Sahli et al also found that the combination of ResNet and SVM realized higher accuracy than ResNet alone in image diagnosis of tumor.[33] In the present study, WRN was used to extract features from the IVD images and derive the T1ρ values as features. The SVM completed the classification task of the IDD phases based on the above T1ρ values. Finally, the model achieved an IDD phases classification accuracy of 0.840. Wu et al found that when using deep learning method to generate T1ρ-MR images from T1- and T2-MR images, the performance was improved compared to single T1/T2-MR image input.[21] Therefore, future study may improve the classification accuracy of T1ρ-MR based IDD phases by incorporating T2-MR images. In summary, the present deep learning model allows the classification of T1ρ-MR based IDD phase using T1-MR images, which reduces time and costs associated with additional T1ρ-MR scanning. Moreover, the recall of phase 2 (rapid degeneration phase) in this model is up to 0.917, and our previous study suggested that intervention during this phase can reverse degeneration.[17] Therefore, efficient screening of patients during this phase may provide treatment opportunities.

Limitations

First, the diversity of dataset is insufficient. The included patients were generally young, and more elderly patients were not included. The training and test data were sourced from a single manufacture MR machine. Additionally, external test datasets were not included. Although we tested the reproducibility of the model using a 5-folds cross validation, it still needs further testing on other datasets. Second, our model can only classify T1ρ-MR based IDD phases from T1-MR images but cannot calculate accurate T1ρ values, which may be related to the small dataset. Third, the model located IVDs in rectangular box form, thus incorporating surrounding structures of the nucleus pulposus, which adds invalid image features and may have a negative impact on the accuracy of IDD phases classification.

Conclusion

The proposed deep learning model can automatically locate the region of lumbar IVDs and further classify T1ρ-MR based IDD phases from routine T1-MR images, which may reduce the additional scanning time and cost of T1ρ-MR for patients and provide a new method to facilitate the application of T1ρ-MR in IDD.

Acknowledgments

Yanrun Li wrote the present paper and measured MR data. Meiyu Hu collected MR images and measured MR data. Junhong Chen built the present deep learning model and conducted training and testing. Zemin Ling and Xuenong Zou provided beneficial suggestions during the study process. Wuteng Cao and Fuxin Wei conceived the idea and planned this study. Thanks to Ximin Pan for providing help in data collection. This study was supported by National Natural Science Foundation of China (82272534, 81972135, and 82102520), National Natural Science Foundation of Guangdong Province (2021A1515010335), Funds for Basic and Applied Basic Research of Guangdong Province (2021B1515140056), Funds for Shenzhen Social Science and Technology Development (JCYJ20190812093401685), Funds for Part-time principal investigator of the Seventh affiliated hospital of Sun Yat-sen University (ZSQYJZPI202005), Sanming Project of Medicine in Shenzhen (SZSM20 1911002), and Shenzhen Key Laboratory of Bone Tissue Repair and Translational Research (ZDSYS202306 26091402006).

Conflict of Interest

The authors have declared that no competing interests exist.

Ethics Statement

This study was approved by the institutional review board of the First Affiliated Hospital of Sun Yat-sen University (certificate no. [2022]563), informed consent was waived for a retrospective analysis.

References

1. Rubin DI. Epidemiology and risk factors for spine pain. Neurol Clin 2007;25(2):353-371.
2. Katz JN. Lumbar disc disorders and low-back pain: Socioeconomic factors and consequences. J Bone Joint Surg Am 2006;88(Suppl 2):21-24.
3. Ricci JA, Stewart WF, Chee E, Leotta C, Foley K, Hochberg MC. Back pain exacerbations and lost productive time costs in United States workers. Spine 2006;31(26):3052-3060.
4. Zhang S, Hu B, Liu W, et al. The role of structure and function changes of sensory nervous system in intervertebral disc-related low back pain. Osteoarthr Cartil 2021;29(1):17-27.
5. Ahn Y. Endoscopic spine discectomy: Indications and outcomes. Int Orthop 2019;43(4):909-916.
6. Benzakour T, Igoumenou V, Mavrogenis AF, Benzakour A. Current concepts for lumbar disc herniation. Int Orthop 2019;43(4):841-851.
7. Toyone T, Tanaka T, Kato D, Kaneyama R. Low-back pain following surgery for lumbar disc herniation. A prospective study. J Bone Joint Surg Am 2004;86(5):893-896.
8. Zhao Y, Qiu C, Wang W, et al. Cortistatin protects against intervertebral disc degeneration through targeting mitochondrial ROS-dependent NLRP3 inflammasome activation. Theranostics 2020;10(15):7015-7033.
9. Pfirrmann CW, Metzdorf A, Zanetti M, Hodler J, Boos N. Magnetic resonance classification of lumbar intervertebral disc degeneration. Spine 2001;26(17):1873-1878.
10. Videman T, Battié MC, Gibbons LE, Gill K. A new quantitative measure of disc degeneration. Spine J 2017;17(5):746-753.
11. Lotz JC, Haughton V, Boden SD, et al. New treatments and imaging strategies in degenerative disease of the intervertebral disks. Radiology 2012;264(1):6-19.
12. Serai SD. Basics of magnetic resonance imaging and quantitative parameters T1, T2, T2*, T1rho and diffusion-weighted imaging. Pediatr Radiol 2022;52(2):217-227.
13. Akella SV, Regatte RR, Gougoutas AJ, et al. Proteoglycan-induced changes in T1rho-relaxation of articular cartilage at 4T. Magn Reson Med 2001;46(3):419-423.
14. Johannessen W, Auerbach JD, Wheaton AJ, et al. Assessment of human disc degeneration and proteoglycan content using T1rho-weighted magnetic resonance imaging. Spine 2006;31(11):1253-1257.
15. Pearce RH, Grimmer BJ, Adams ME. Degeneration and the chemical composition of the human lumbar intervertebral disc. J Orthop Res 1987;5(2):198-205.
16. Zhou Z, Jiang B, Zhou Z, et al. Intervertebral disk degeneration: T1ρ MR imaging of human and animal models. Radiology 2013;268(2): 492-500.
17. Liu Z, Li J, Hu M, et al. The optimal timing of hydrogel injection for treatment of intervertebral disc degeneration: Quantitative analysis based on T1ρ MR imaging. Spine 2020;45(22):E1451-E1459.
18. Wang L, Regatte RR. $T_1\rho$ MRI of human musculoskeletal system. J Magn Reson Imaging 2015;41(3):586-600.
19. Hallinan JTPD, Zhu L, Yang K, et al. Deep learning model for automated detection and classification of central canal, lateral recess, and neural foraminal stenosis at lumbar spine MRI. Radiology 2021;300(1): 130-138.

20. Jans LBO, Chen M, Elewaut D, et al. MRI-based synthetic CT in the detection of structural lesions in patients with suspected sacroiliitis: Comparison with MRI. Radiology 2021;298(2):343-349.
21. Wu Y, Li D, Xing L, Gold G. Deriving new soft tissue contrasts from conventional MR images using deep learning. Magn Reson Imaging 2020;74:121-127.
22. Shrout PE. Measurement reliability and agreement in psychiatry. Stat Methods Med Res 1998;7(3):301-317.
23. Vianna P, Calce S-I, Boustros P, et al. Comparison of radiologists and deep learning for US grading of hepatic steatosis. Radiology 2023; 309(1):e230659.
24. Niemeyer F, Galbusera F, Tao Y, Kienle A, Beer M, Wilke HJ. A deep learning model for the accurate and reliable classification of disc degeneration based on MRI data. Invest Radiol 2021;56(2):78–85.
25. Zheng H-D, Sun Y-L, Kong D-W, et al. Deep learning-based high-accuracy quantitation for lumbar intervertebral disc degeneration from MRI. Nat Commun 2022;13(1):841.
26. Fang Y, Li W, Chen X, et al. Opportunistic osteoporosis screening in multi-detector CT images using deep convolutional neural networks. Eur Radiol 2021;31(4):1831-1842.
27. Tsai J-Y, Hung IY-J, Guo YL, et al. Lumbar disc herniation automatic detection in magnetic resonance imaging based on deep learning. Front Bioeng Biotechnol 2021;9:708137.
28. Liawrungrueang W, Kim P, Kotheeranurak V, Jitpakdee K, Sarasombath P. Automatic detection, classification, and grading of lumbar intervertebral disc degeneration using an artificial neural network model. Diagnostics 2023;13(4):663.
29. Prisilla AA, Guo YL, Jan Y-K, et al. An approach to the diagnosis of lumbar disc herniation using deep learning models. Front Bioeng Biotechnol 2023;11:1247112.
30. Ito S, Nakashima H, Segi N, et al. Automated detection and diagnosis of spinal schwannomas and meningiomas using deep learning and magnetic resonance imaging. J Clin Med 2023;12(15):5075.
31. Zagoruyko S, Komodakis N. Wide residual networks. *arXiv*2016.
32. Zhou C, Song J, Zhou S, Zhang Z, Xing J. COVID-19 detection based on image regrouping and Resnet-SVM using chest X-ray images. IEEE Access 2021;9:81902-81912.
33. Sahli H, Ben Slama A, Zeraii A, Labidi S, Sayadi M. ResNet-SVM: Fusion based glioblastoma tumor segmentation and classification. J Xray Sci Technol 2023;31(1):27-48.